Stem Cell Reports
Report
OPEN ACCESS

Identification of the Common Origins of Osteoclasts, Macrophages, and Dendritic Cells in Human Hematopoiesis

Yanling Xiao,[1,*] Sebastiaan Zijl,[1] Liqin Wang,[1] Daniel C. de Groot,[1] Maarten J. van Tol,[2] Arjan C. Lankester,[2] and Jannie Borst[1,*]
[1]Division of Immunology, The Netherlands Cancer Institute-Antoni van Leeuwenhoek, Amsterdam 1066 CX, the Netherlands
[2]Division of Stem Cell Transplantation, Department of Pediatrics, Leiden University Medical Center, Leiden 2300 RC, the Netherlands
*Correspondence: y.xiao@nki.nl (Y.X.), j.borst@nki.nl (J.B.)
http://dx.doi.org/10.1016/j.stemcr.2015.04.012

SUMMARY

Osteoclasts (OCs) originate from the myeloid cell lineage, but the successive steps in their lineage commitment are ill-defined, especially in humans. To clarify OC origin, we sorted cell populations from pediatric bone marrow (BM) by flow cytometry and assessed their differentiation potential in vitro. Within the $CD11b^{-}CD34^{+}c\text{-}KIT^{+}$ BM cell population, OC-differentiation potential was restricted to $FLT3^{+}$ cells and enriched in an IL3 receptor (R)α^{high} subset that constituted less than 0.5% of total BM. These IL3Rα^{high} cells also generated macrophages (MΦs) and dendritic cells (DCs) but lacked granulocyte (GR)-differentiation potential, as demonstrated at the clonal level. The IL3Rα^{low} subset was re-defined as common progenitor of GR, MΦ, OC, and DC (GMODP) and gave rise to the IL3Rα^{high} subset that was identified as common progenitor of MΦ, OC, and DC (MODP). Unbiased transcriptome analysis of $CD11b^{-}CD34^{+}c\text{-}KIT^{+}FLT3^{+}$ IL3Rα^{low} and IL3Rα^{high} subsets corroborated our definitions of the GMODP and MODP and their developmental relationship.

INTRODUCTION

Osteoclasts (OCs), macrophages (MΦs), and dendritic cells (DCs) are closely related cells of the myeloid lineage (Arai et al., 1999). Terminally differentiated OCs fuse to form large, multinucleated cells that resorb bone. OCs differentiate from precursors under influence of RANK ligand (L) that is produced by bone-forming osteoblasts. Ordinarily, OCs and osteoblasts thus maintain bone homeostasis in a balanced interaction (Theill et al., 2002). However, in cancer and autoimmune and inflammatory diseases, OC formation can be promoted by RANKL-expressing tumor or immune cells, which facilitates bone metastasis, pathological bone loss, and remodeling (Walsh et al., 2006). Although OCs are of key importance, their developmental pathway is largely unknown as testified by the striking absence of OCs in most depictions of the hematopoietic tree.

The hematopoietic tree describes the developmental pathways of all blood cells emanating from the pluripotent hematopoietic stem cell (HSC). The self-renewing HSC yields the multipotent progenitor (MPP), which in turn gives rise to more lineage-restricted, oligopotent precursors. The classical model dictates that the MPP bifurcates into a common myeloid progenitor (CMP) and a common lymphoid progenitor (CLP). The CMP in turn would bifurcate into the megakaryocyte/erythrocyte progenitor (MEP) and the granulocyte (GR)/MΦ progenitor (GMP). GRs, monocytes/MΦs, and DCs were thought to arise downstream of the GMP (Weissman and Shizuru, 2008). However, in an alternative model based on mouse data, the MPP bifurcates into a precursor with megakaryocyte/erythroid potential and one with combined myeloid and lymphoid potential (Kawamoto et al., 2010). This myeloid-based model was supported by the identification of a murine lympho/myeloid precursor (LMPP) devoid of megakaryocyte/erythroid potential (Adolfsson et al., 2005). Also in line with the myeloid-based model was the identification of a human multilymphoid progenitor (MLP) that gave rise to lymphoid cells, MΦs, and DCs (Doulatov et al., 2010). This MLP replaced the CLP in the scheme of human hematopoiesis (Doulatov et al., 2012). In the proposed scenario, both MLP and GMP can yield MΦs and DCs, whereas the GMP can additionally give rise to GRs (Figure 1A). Findings in humans also supported the existence of the LMPP (Goardon et al., 2011) and suggested that it bifurcates into the MLP and the GMP (Görgens et al., 2013; Figure 1A). Recent data in human also revise the view on the CMP, in accordance to findings in the mouse (Kawamoto et al., 2010): the human MPP was found to yield a common erythro-myeloid progenitor (EMP) that gives rise to the MEP and to a precursor of eosinophilic and basophilic GRs (EoBP) (Mori et al., 2009; Görgens et al., 2013). In the revised scheme, the CMP is absent and the GMP lies downstream of the LMPP (Figure 1A).

The human GMP was found to yield only neutrophils and not other types of GRs (Görgens et al., 2013). Exactly how monocytes/MΦs and DCs develop downstream of the GMP is intensely studied both in human and mouse. In the mouse, a common monocyte/MΦ/DC progenitor (MDP) has been proposed. The MDP is thought to give rise to a common DC progenitor (CDP) that exclusively forms plasmacytoid and conventional DCs and to a

common monocyte progenitor (cMoP) that exclusively forms monocytes and MΦs (Liu and Nussenzweig, 2010; Hettinger et al., 2013). In contrast, little attention is paid to OC development. Seminal studies in the mouse have demonstrated that OCs, MΦs, and DCs derive from a common MΦ/OC/DC progenitor (MODP) that lies downstream of the GMP (Arai et al., 1999; Miyamoto et al., 2001), as confirmed by others (Jacome-Galarza et al., 2013). However, equivalent findings on the origin of the OC in human hematopoiesis have thus far not been reported.

We previously examined the fate of OC precursors in mouse BM. Herein, we confirmed and refined the earlier definition of the MODP and found a downstream MOP (Xiao et al., 2013). Using the methodology and cues from this mouse study, we searched for the MODP in humans and report it here.

RESULTS AND DISCUSSION

OC Precursors Are Enriched in the CD11b$^-$CD34$^+$c-KIT$^+$FLT3$^+$ IL3Rα^{high} Fraction of Human BM

To identify human OC precursors, we flow cytometrically purified bone marrow (BM) populations from healthy pediatric donors (Table S1) and analyzed their differentiation potential in vitro. As markers, we used presence of CD34 as progenitor marker and, by analogy with the mouse MODP, presence of c-KIT (CD117) and absence of CD11b (Arai et al., 1999; Xiao et al., 2013). We also examined FLT3 (CD135) as potential marker, because it is on the mouse MODP (Figure S1A). The tyrosine kinase receptor FLT3 is essential for homeostatic DC development (McKenna et al., 2000). It is expressed on the CDP and on upstream precursors in the mouse (Liu and Nussenzweig, 2010; Weissman and Shizuru, 2008), where high FLT3 levels distinguish the mouse LMPP from the MEP (Adolfsson et al., 2005). Among CD11b$^-$ BM cells, we identified CD34$^{-/low}$c-KIT$^+$ (G1), CD34$^+$c-KIT$^+$ (G2), and CD34$^+$c-KIT$^-$ (G3) populations, of which G2 and G3 could be separated into FLT3$^-$ (a) and FLT3$^+$ (b) subpopulations (Figure 1B). Among these five populations, only CD34$^+$c-KIT$^+$FLT3$^+$ (G2b) cells proved to have OC-differentiation potential (Figure S1B). Mature OCs were identified by positive staining for tartrate-resistant acid phosphatase (TRAP) and vitronectin receptor (Figure S1C) and by a multi-nuclear appearance (Figure 1C).

To narrow down the OC precursor population, we tested as additional markers c-FMS (alias CSF1R/CD115); the M-CSF receptor for that is present on the MODP (Arai et al., 1999) and on designated DC and MΦ precursors in the mouse (Liu and Nussenzweig, 2010; Hettinger et al., 2013). *CSF1R* mRNA was present in CD34$^+$c-KIT$^+$FLT3$^+$ precursor cells (Figure 1D), but we could not detect the protein at the cell surface (results not shown). We also tested CD27 that marks the murine MODP (Xiao et al., 2013; Figure S1A), but it was not synthesized in CD11b$^-$CD34$^+$c-KIT$^+$FLT3$^+$ BM cells (Figure 1D). We next considered IL3Rα (CD123), because its mRNA was enriched in the FLT3$^+$ fraction of CD11b$^-$CD34$^+$c-KIT$^+$ human BM cells (Figure 1D) and it discriminates CMP and GMP from MEP (Mori et al., 2009). IL3Rα cell surface expression separated CD11b$^-$CD34$^+$c-KIT$^+$FLT3$^+$ BM cells into two populations: ~70%–80% had an IL3Rα^{low} phenotype and the rest had an IL3Rα^{high} phenotype (Figure 1E). These populations corresponded to ~1.7% and ~0.5%, respectively, of live, ficolled BM cells (Figure 1F).

Both precursor populations were negative for a lineage (Lin) marker set composed of CD2, CD3, CD14, CD16, CD19, CD56, and CD235a (Figure 1E). They also lacked CD7 and CD10 (Figure 1D; results not shown) that are acquired at the level of the MLP. They expressed CD38 (Figure 1G) that is acquired downstream of the MPP (Doulatov et al., 2010). The Lin$^-$CD7$^-$CD10$^-$CD34$^+$CD38$^+$IL3Rα^{low} human BM population can be divided into a CD45RA$^+$ subset that contains the GMP and a more upstream CD45RA$^-$ subset with additional MEP potential (Manz et al., 2002). CD45RA is also expressed on the MLP, but not further upstream (Doulatov et al., 2010). Within the CD11b$^-$CD34$^+$c-KIT$^+$FLT3$^+$population, the IL3Rα^{high} subset was uniformly CD45RA$^+$ and the IL3Rα^{low} subset was largely CD45RA$^+$ (Figure 1G), suggesting that they resided at the level of, or downstream from, the GMP or MLP. The IL3Rα^{low} and IL3Rα^{high} subsets were tested for OC-differentiation potential. Only the IL3Rα^{high} cells grew out and formed multi-nuclear TRAP$^+$ OC, whereas IL3Rα^{low} cells formed low numbers of mono-nuclear TRAP$^+$ OCs that were apparently less mature (Figures 1H and 1I). We conclude that human OC-precursor potential is enriched within the CD11b$^-$CD34$^+$c-KIT$^+$FLT3$^+$IL3Rα^{high} BM population that is furthermore Lin$^-$CD7$^-$CD10$^-$CD38$^+$CD45RA$^+$ and constitutes less than 0.5% of total pediatric BM.

Positioning of the IL3Rα^{low} and IL3Rα^{high} Subsets of CD11b$^-$CD34$^+$c-KIT$^+$FLT3$^+$ BM Cells Relative to the GMP and MLP

To determine the position of the IL3Rα^{low} and IL3Rα^{high} subsets of CD11b$^-$CD34$^+$c-KIT$^+$FLT3$^+$ BM cells relative to the GMP, we evaluated their potential to form GRs. Interestingly, the IL3Rα^{low} subset abundantly generated GRs, whereas the IL3Rα^{high} subset lacked this potential (Figures 2A–2C). To position the IL3Rα^{low} and IL3Rα^{high} subsets relative to the MLP, we evaluated their potential to generate B cells. Neither subset yielded B cells, whereas CD34$^+$c-KIT$^-$ cells—which contain CD10$^+$ precursors (results not shown)—did, which validated the assay (Figure 2D).

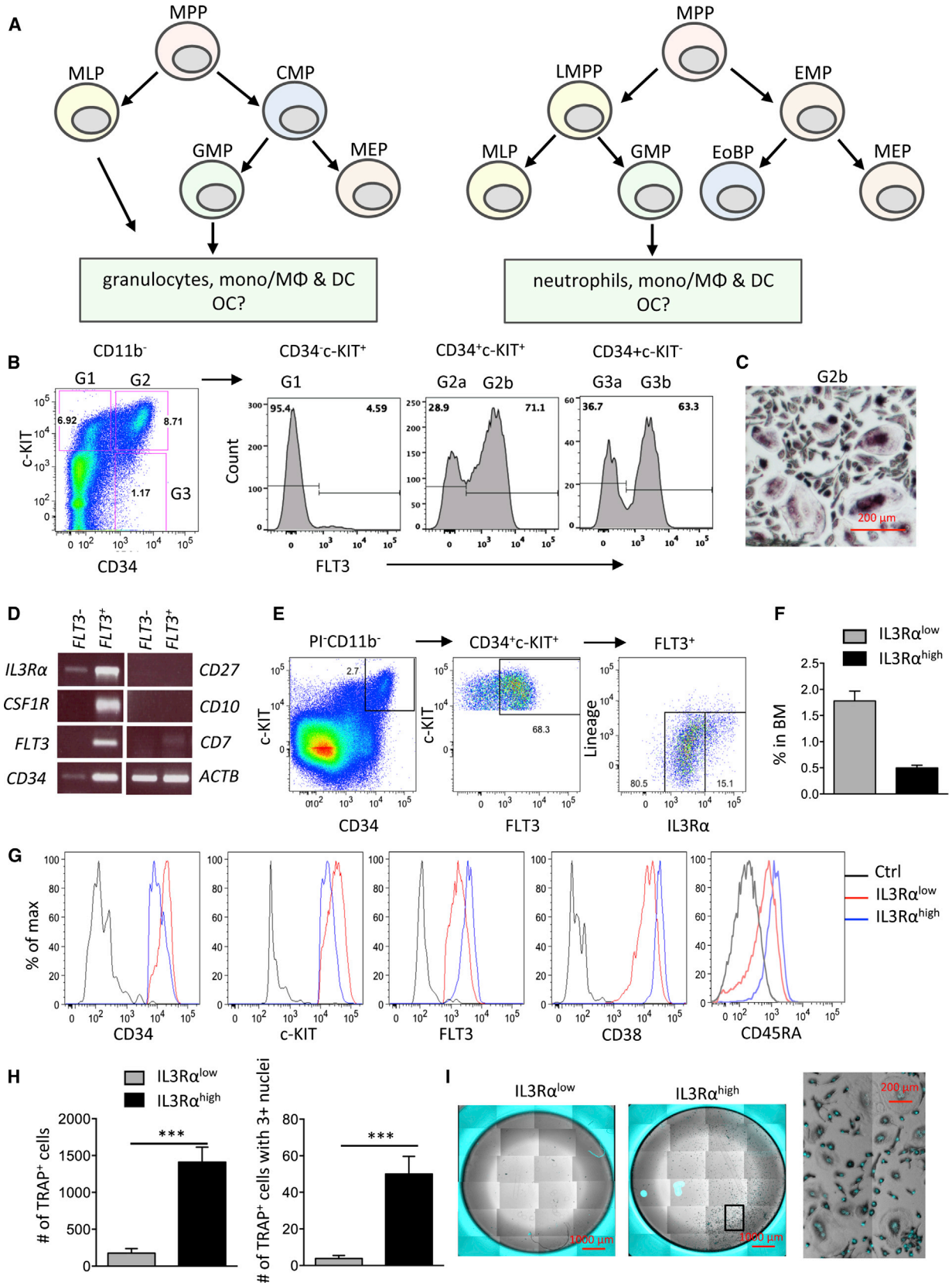

(legend on next page)

We next examined MΦ-differentiation potential. The IL3Rα^{high} subset was more efficient at MΦ formation than the IL3Rα^{low} subset (Figures 2E–2G). When plated at 1,000 cells per well, the IL3Rα^{high} subset generated 7,000–10,000 cells over 14 days (Figure 2F), most of which were MΦs as indicated by a CD14^{+}CD68^{+} phenotype (Figure 2G). Yield from IL3Rα^{low} precursors tended to be lower (Figures 2F and 2G). The difference was not statistically significant but consistent for multiple BM samples in 8- or 14-day cultures (data not shown).

To examine DC-differentiation potential, the IL3Rα^{low} and IL3Rα^{high} subsets were cultured with M-CSF and FLT3L. After 8 or 14 days of culture, the IL3Rα^{low} subset generated more offspring than the IL3Rα^{high} subset (Figures 2H and 2I). However, the IL3Rα^{high} subset was significantly more efficient at generating CD11c^{+} HLA-DR^{+} cells than the IL3Rα^{low} subset in the time frame of culture (Figure 2I). Within the CD11c^{+} HLA-DR^{+} population, CD1c (BDCA-1) and CD141 (BDCA-3) were expressed that are proposed markers of conventional (c)DCs (MacDonald et al., 2002; Figure 2J). CD303 (BDCA-2) that is a marker for plasmacytoid (p)DCs (MacDonald et al., 2002) was not detected (data not shown).

Our data argue that, among CD11b^{-}CD34^{+}c-KIT^{+}FLT3^{+} human BM cells, the IL3Rα expression level discriminates two successive stages in commitment toward the OC, MΦ, and DC fate. The IL3Rα^{low} subset defines the GMP (Manz et al., 2002), but we propose that this subset should be re-defined as GR, MΦ, OC, and DC progenitor (GMODP). The IL3Rα^{high} subset is candidate for the downstream, newly defined human MODP.

Validation of the IL3Rα^{low} and IL3α^{high} Subsets as GMODP and MODP by Refined Analysis of DC and MΦ Offspring and Clonal Analysis of Oligopotency

To validate that the IL3Rα^{high} subset of CD11b^{-}CD34^{+}c-KIT^{+}FLT3^{+} BM cells qualified as DC progenitor, we analyzed the offspring with more-specific markers for DCs, using the study by Balan et al. (2014) as a guideline. These authors recently proved able to derive XCR1^{+} DCs from human CD34^{+} cord blood cells, using a cytokine cocktail and a feeder cell layer. Importantly, they showed by transcriptome analysis that these DCs were highly similar to primary XCR1^{+} DCs from blood and distinct from monocyte-derived DCs. The CD34^{+} cells in culture also generated XCR1^{-} DCs that were similar to monocyte-derived DCs. In a side-by-side comparison, we found that MΦ and DC cultures from IL3Rα^{high} subset contained similar amounts of CD11b^{+} HLA-DR^{+} cells and that virtually all cells in both cultures expressed CD141 (Figure S2A). XCR1- and Clec9a-expressing cells were clearly enriched in the DC culture as compared to the MΦ culture (Figure 3A). This agrees with Balan et al. (2014), who identified XCR1 and Clec9a, but not CD141, as markers that discriminate between progenitor-derived DCs and monocyte-derived DCs. The DC culture contained more XCR1^{+}Clec9a^{+} cells than the MΦ culture (Figure 3B), and these cells were enriched for the DC markers FLT3 and CD1c. In the MΦ culture, XCR1^{+}Clec9a^{+} cells were enriched for the MΦ marker CD14^{high} (Figure 3B). The XCR1^{-}Clec9a^{-} cells in the DC culture also differed from those in the MΦ culture (Figure 3C). In the DC culture, a large proportion of XCR1^{-}Clec9a^{-} expressed the DC markers FLT3 and/or CD1c, but this was not the case in the MΦ culture. Moreover, in the MΦ culture, the XCR1^{-}Clec9a^{-} cells were uniformly CD14^{high}, but this was not the case in the DC culture. Furthermore, the discriminatory monocyte/MΦ marker *FCGR2A* (Balan et al., 2014) was enriched in the MΦ cultures as compared to the DC cultures (Figure S2B), and cells from the MΦ cultures had a much greater ability to phagocytose beads than cells from the DC cultures (Figure S2C). Thus, the IL3α^{high} subset gives rise to distinct progenies under DC- versus MΦ-differentiation conditions, arguing that it is a common progenitor for DCs and MΦs.

Figure 1. Identification of OC Progenitors in Human BM

(A) Proposed models of hematopoietic development, as based on Doulatov et al. (2012) (left) and Görgens et al. (2013) (right). OC origin is proposed by us.

(B) Gating strategy for sorting of the live, CD11b^{-} G1, G2a and b, and G3a and b populations from ficolled BM.

(C) Light microscopic image showing TRAP^{+} multi-nuclear OC derived from the G2b population.

(D) RT-PCR-based mRNA expression of the indicated genes defined in the FLT3^{-} (G2a) and FLT3^{+} (G2b) subsets of CD11b^{-}CD34^{+}c-KIT^{+} BM cells.

(E) Gating for sorting live (PI^{-}), IL3Rα^{low}, and IL3Rα^{high} CD11b^{-}CD34^{+}c-KIT^{+}FLT3^{+} cells from ficolled BM and lineage marker analysis.

(F) The contribution (%) of the subsets to the total number of live cells in ficolled BM (mean + SEM; seven donors).

(G) Flow cytometric detection of the indicated markers on the IL3Rα^{low} and IL3Rα^{high} subsets (Ctrl, unstained IL3Rα^{low} samples), representative of three donors.

(H and I) OC differentiation of IL3Rα^{low} and IL3Rα^{high} subsets was analyzed at days 7–9. (H) OC differentiation was quantified as number (#) per well of (left) all TRAP^{+} cells and (right) TRAP^{+} cells with more than three nuclei (mean + SEM; five donors; ***$p < 0.001$). (I) The phenotypic appearance of TRAP-stained OC cultures was determined by CCD microscopy. Green, DAPI staining of nuclei; gray/black, TRAP staining.

See also Figure S1.

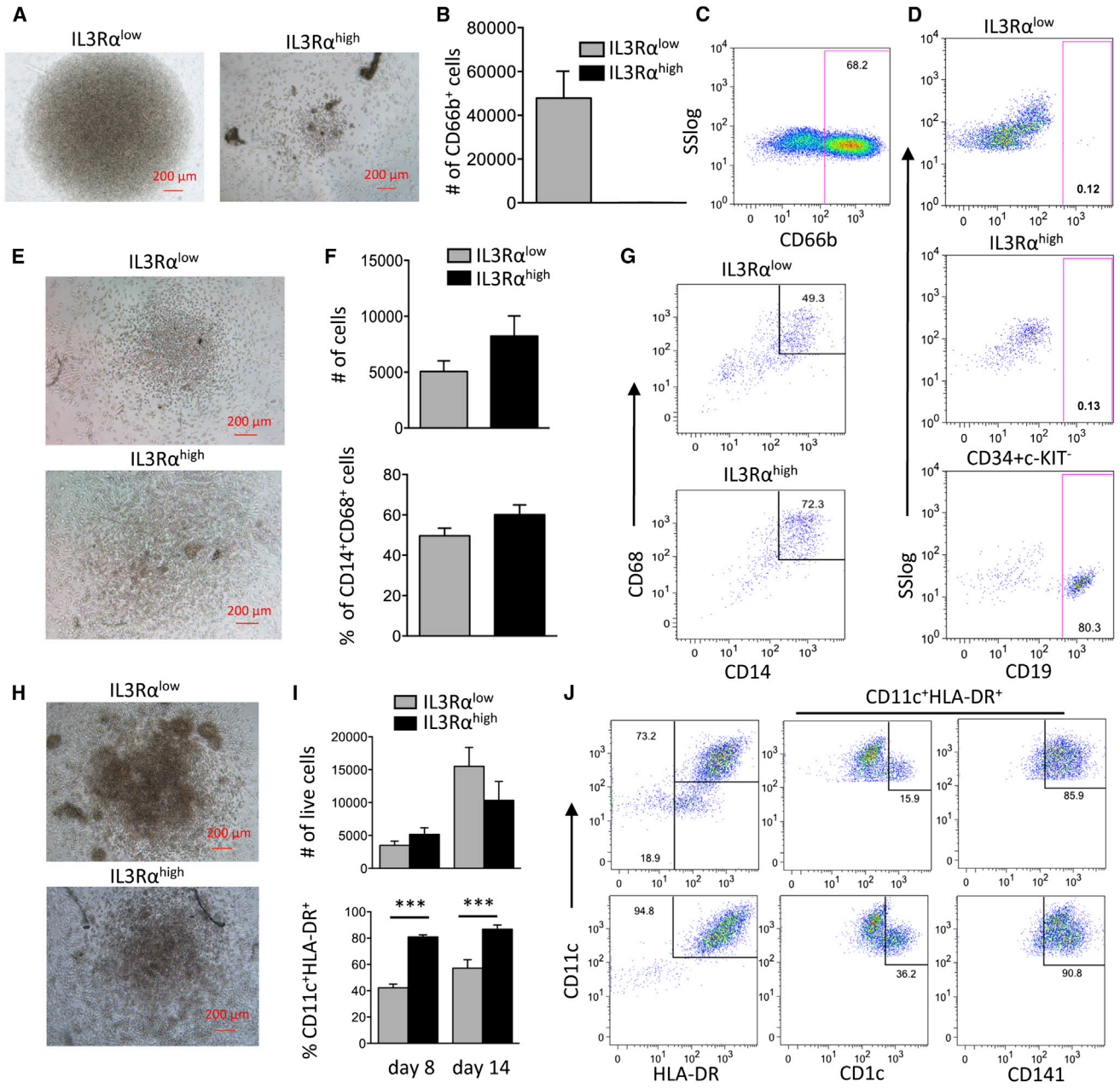

Figure 2. Positioning of the IL3Rα^{low} and IL3Rα^{high} CD11b^{-}CD34^{+}c-KIT^{+}FLT3^{+} BM Subsets Relative to the GMP and MLP

The IL3Rα^{low} and IL3Rα^{high} subsets of CD11b^{-}CD34^{+}c-KIT^{+}FLT3^{+} BM cells were sorted and cultured at 1,000 cells/well to determine GR-, B-cell-, MΦ-, and DC-differentiation potential.

(A–C) GR differentiation was analyzed at day 14. (A) Appearance of cultures was determined by light microscopy. (B) Absolute number (#) of live (PI^{-}) GRs was determined by flow cytometry based on CD66b expression (mean + SEM; five donors). (C) Representative diagnosis of CD66b expression is depicted (SS, side scatter).

(D) B cell differentiation. After 3 to 4 weeks of culture, B cells were defined by flow cytometric detection of CD19. Sorted CD34^{+}c-KIT^{-} cells were cultured as a positive control. Data are representative of seven donors.

(E–G) MΦ differentiation was analyzed at day 14. (E) Appearance of cultures was determined by light microscopy. (F) Absolute number (#) of cells in culture and frequency (%) of CD14^{+}CD68^{+} cells was determined by flow cytometry (mean + SEM; five donors). (G) Representative diagnosis of CD14 and CD68 expression is depicted.

(legend continued on next page)

Oligopotency of the progenitors was tested in clonogenic assays. From the IL3Rα^{low} subset, but not from the IL3Rα^{high} subset, single cells could be expanded with cytokines on a mesenchymal stem cell layer (Figure 3D). The offspring of a single IL3Rα^{low} progenitor could generate MΦs, OCs, or DCs, under the respective differentiation conditions (Figure 3E), indicating its multi-lineage potential. When plated as single cells directly after sorting, the IL3Rα^{low} subset yielded MΦs, DCs, and GRs, whereas the IL3Rα^{high} subset gave rise to MΦs and DCs, but not GRs (Figures S2D and S2E). OCs did not emerge in either situation, presumably because of the demanding single-cell culture. The single-cell cultures also did not yield B cells, as expected from the results of the bulk cultures (Figure S2D). Our data argue that, among CD11b$^-$CD34$^+$c-KIT$^+$FLT3$^+$ human BM cells, the IL3Rα expression level discriminates between two successive stages in commitment toward MΦ, OC, and DC differentiation. The IL3Rα^{low} subset of this BM population constitutes the GMODP, oligopotent for GR, MΦ, OC, and DC differentiation. The IL3Rα^{high} subset lies downstream from the GMODP and constitutes the newly identified MODP, which is oligopotent for MΦ, OC, and DC differentiation (Graphical Abstract).

mRNA Deep Sequencing Supports the Proposed GMODP-MODP Relationship between the IL3Rα^{low} and IL3Rα^{high} Subsets of CD11b$^-$CD34$^+$c-KIT$^+$FLT3$^+$ BM Cells

To further define the IL3Rα^{high} and IL3Rα^{low} subsets and their relationship, we compared their gene-expression profiles. The transcriptome of 10,000–20,000 cells per sample (n = 3) was successfully determined by mRNA deep sequencing. Analysis of all protein-coding genes showed that the IL3Rα^{high} samples clustered together, as did the IL3Rα^{low} samples (Figure 4A). This confirmed the discriminatory potential of the IL3Rα marker. At $p < 0.001$, 649 protein-coding genes were differentially expressed between the two subsets, indicating their close relationship but distinct nature. Among these, 97 genes with the highest level of differential expression were used to make a heatmap that specifies the distinct nature of the two subsets (Figure 4B). Furthermore, the 649 differentially expressed protein-coding genes were analyzed by ingenuity pathway analysis (IPA). Gene clusters upregulated in the IL3Rα^{high} subset included the functional categories "differentiation of MΦs," "differentiation of OCs," and "differentiation of antigen-presenting cells" (Figure 4C), indicating a further commitment to MΦ/OC/DC differentiation in the transition from the IL3Rα^{low} to the IL3Rα^{high} phenotype. Gene clusters downregulated in the IL3Rα^{high} subset included the functional categories "differentiation of B lymphocytes," "quantity of granulocytes," and "quantity of eosinophils," consistent with differentiation away from the GR fate (Figure 4C). In addition, a gene cluster denoting "differentiation of cells" was upregulated and a gene cluster denoting "proliferation of hematopoietic progenitor cells" was downregulated, in accordance with further commitment to a differentiated cell fate (Figure 4C). The IL3Rα^{high} subset showed higher mRNA expression of transcription factors important for pDC, cDC, and MΦ development, including *SPIB*, *IRF4*, *IRF8*, *SPI1/PU.1*, and *ID2* (Figures 4C and 4D; Belz and Nutt, 2012; Lawrence and Natoli, 2011; Rosenbauer and Tenen, 2007). This indicated that both pDC and cDC developmental capacity is contained within the human MODP. Furthermore, in the IL3Rα^{high} subset, *CSF1R* was upregulated (Figure 4D), as well as *OSCAR*, *TYROBP* (*DAP12*), and *SYK* (Figure 4C), a membrane receptor and signaling molecules that drive OC differentiation (Takayanagi, 2007). Both IL3Rα^{high} and IL3Rα^{low} precursor populations expressed myeloperoxidase (MPO) that is diagnostic for the GMP (Manz et al., 2002) at similarly high levels (Figure 4D). Collectively, these deep-sequencing data strongly support, in an unbiased fashion, our phenotypic and functional definitions of the human GMODP and MODP.

Whereas this paper was in the final stage of revision, Lee et al. (2015) published on the origin of DCs and MΦs in human hematopoiesis. In human cord blood, they separated the CD34$^+$CD38^{high}CD45RA$^+$CD10$^-$ cell population into IL3Rα^{int} and IL3Rα^{high} subsets that were both FLT3 positive. Within the IL3Rα^{int} subset, they re-defined a CD115$^-$CD116$^-$ population as GMDP, i.e., a precursor that has DC-differentiation potential in addition to previously determined GR- and MΦ-differentiation potential. We show that the CD11b$^-$CD34$^+$c-KIT$^+$FLT3$^+$ population in pediatric BM is Lin$^-$CD38$^+$CD45RA$^+$CD10$^-$, and we also find no CD115 (c-FMS/CSFR1) on the cell surface of the IL3Rα^{low} subset of this population. Thus, we agree on the identity of the GMDP and reveal that it is in fact a GMODP. Furthermore, Lee et al. (2015) defined within the IL3Rα^{int} subset a CD115$^+$CD116$^-$ population as MDP, i.e., a precursor that can give rise to DCs and MΦs, but not GRs. The CD115$^-$IL3Rα^{high} subset was defined as CDP, i.e., a dedicated common precursor of cDC and pDC. In absence of a direct comparison of the cord blood and pediatric BM populations, we cannot exactly match the proposed MDP and CDP to our MODP. Both cord blood

(H–J) DC differentiation was analyzed at day 8 or 14. (H) Appearance of cultures was determined by light microscopy at day 8. (I) Absolute number (#) of live cells and frequency (%) of CD11c$^+$ HLA-DR$^+$ cells was determined by flow cytometry (mean + SEM; five donors; ***$p < 0.001$). (J) Representative diagnosis is depicted of CD11c and HLA-DR within the live-cell gate and CD1c and CD141 within the CD11c$^+$HLA-DR$^+$ gate.

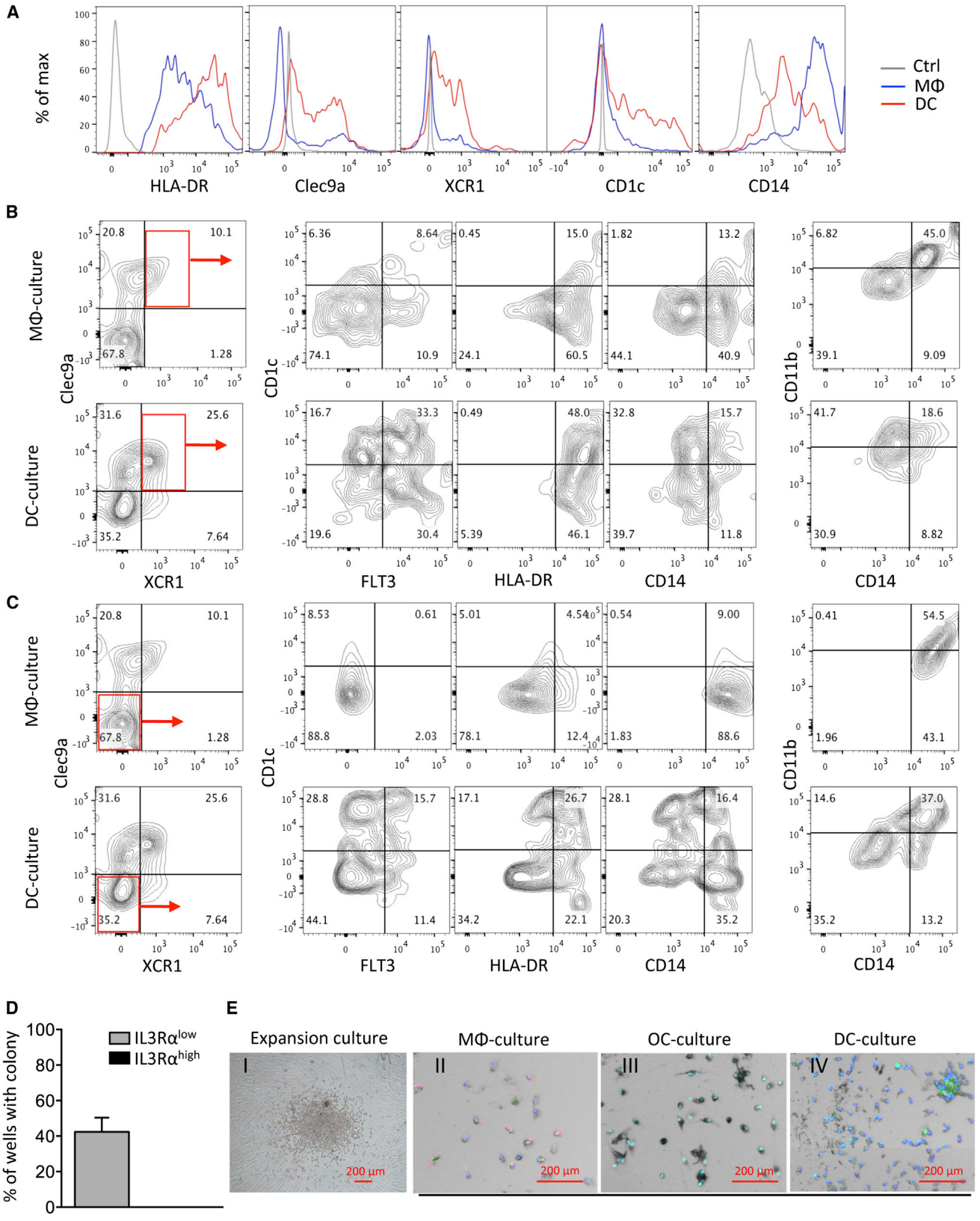

(legend on next page)

populations should be tested for OC potential. Also, the CDP population should be tested for MΦ-differentiation potential with M-CSF, because only GM-CSF was used. Nevertheless, we fully agree that an M(O)DP exists downstream of the GM(O)DP. Lee et al. (2015) proved both pDC and cDC potential of their precursors by deep sequencing of culture-derived and primary cells, supporting the common DC potential revealed by deep sequencing in our MODP. Future work should address the functionality of the culture-derived cells. Also, additional markers must be found to discern the MODP and proposed CDP. Understanding the development of OC, DC, and MΦ is important for clinical diagnostics, targeted drug-based therapy, and cellular therapy. Identification of the MODP will also facilitate generation of these cell types, with precursor stemness benefitting expansion and cell yield.

EXPERIMENTAL PROCEDURES

Human BM and Flow Cytometry

BM was obtained from healthy children that were donors for their sibling, with approval of the medical ethical committee of Leiden University Medical School (protocol P08.001) and with parental informed consent. BM mono-nuclear cells were isolated by density gradient centrifugation on Ficoll and cryopreserved until use. Cells were stained with antibodies in medium with 2% FCS. Prior to sorting, 0.01% deoxyribonuclease I was added to prevent cell clumping and 1 μg/ml propidium iodide (Sigma-Aldrich) to exclude dead cells. Cells were sorted on a FACSAria and analyzed on an LSRFortessa (BD Biosciences) or CyAn (Beckman Coulter Genomics). Data were analyzed with FloJo software. For mAbs used for flow cytometry, see Table S2.

In Vitro Differentiation Cultures

In in vitro differentiation cultures, 1,000 sorted precursor cells were cultured per well in 96-well plates (BD Falcon). Culture conditions were as follows: (1) OC differentiation: 7–9 days in 200 μl of MEM-α with 10% FCS, 25 ng/ml recombinant human (rh) M-CSF, and 40 ng/ml rh RANKL. (2) DC differentiation: 8 or 14 days in IMDM with 10% FCS, 25 ng/ml rh M-CSF, and 200 ng/ml rh FLT3L (and 10 ng/ml IL-3 for the experiment depicted in Figures 3A–3C). For MΦ-, GR-, and B-cell differentiation, cells were cultured on a monolayer of OP9 cells. (3) MΦ differentiation: 8 or 14 days in IMDM with 10% FCS, 25 ng/ml rh M-CSF, and 1,000 U/ml rh IL-6 (Chomarat et al., 2000). (4) GR differentiation: 14 days in IMDM with 10% FCS and 100 ng/ml rh G-CSF (Choi et al., 2009). (5) B-cell differentiation: 3 to 4 weeks in RPMI-1640 with 10% FCS and 15 ng/ml rh IL-7 (Miltenyi Biotech; Vieira and Cumano, 2004). For clonogenic assays, cells were sorted at one cell per well and either pre-expanded in IMDM with 10% FCS and 5 ng/ml SCF, 10 ng/ml TPO, 5 ng/ml M-CSF, and 20 ng/ml Flt3L on a mesenchymal stem cell layer (Xiao et al., 2013) or cultured directly. Growth factors were from R&D Systems unless otherwise indicated. For analysis of cell differentiation, see Supplemental Information.

RNA Deep Sequencing and PCR

For mRNA deep sequencing, 10,000–40,000 precursors were flow cytometrically sorted, dissolved in Trizol reagent (Ambion), and delivered to the NKI Genomics Core Facility. Here, mRNA was isolated and deep sequencing was performed using a HiSeq200 (Illumina). Sequence reads were aligned with TopHat software to the Ensembl gene set *Homo sapiens* GRCh37.66. Reads were counted using htseq-count software. Hierarchical clustering was done in R and uses 1-correlation as the distance function. Reads for protein-coding genes were normalized and analyzed for differential expression using R package limma. The heatmap was generated using Qlucore Omics Explorer software (Qlucore). For real-time (RT) and/or quantitative (q) PCR, RNA was isolated using the RNeasy Mini Kit (QIAGEN) and treated with DNase I (QIAGEN) to remove genomic DNA. Next, cDNA was prepared on a Peltier Thermal Cycler (BioRad), using SuperScript II reverse transcriptase (Invitrogen), and either RT-PCR or qPCR was performed with the primers listed in Table S3. See Supplemental Information for further details.

Statistical Analysis

See Supplemental Information.

ACCESSION NUMBERS

The GEO accession number for the data reported in this paper is GSE65996.

Figure 3. Validation of the IL3Rα^{low} and IL3Rα^{high} Subsets as GMODP and MODP

(A–C) Sorted IL3Rα^{high}CD11b^{-}CD34^{+}c-KIT^{+}FLT3^{+} BM cells were cultured side by side under MΦ- or DC-differentiation conditions and analyzed by flow cytometry on day 12. Data are representative of two donors. (A) Indicated marker expression was determined in gated CD11b^{+}HLA-DR^{+} cells from MΦ (blue line) or DC (red line) cultures. Grey lines depict controls (Ctrl), unstained samples from the DC culture. (B and C) Within gated CD11b^{+}HLA-DR^{+} cells, XCR1^{+}Clec9a^{+} (B) and XCR1^{-}Clec9a^{-} (C) populations were further gated (red boxes in the left panels) and analyzed for indicated markers.

(D and E) Clonal analysis of oligopotency. IL3Rα^{low} and IL3Rα^{high} subsets were cultured at one cell per well with SCF, TPO, M-CSF, and FLT3L on a mesenchymal stem cell layer for 7–10 days (expansion culture). (D) Percentage of wells with a colony was determined out of 48 wells seeded (mean + SEM; two donors). (E) Expansion cultures were split into three equal fractions and further cultured for 7 days under MΦ-, OC-, or DC-differentiation conditions. (I) Colony from IL3Rα^{low} subset in expansion culture was analyzed by light microscopy. (II–IV) Cells generated were visualized by fluorescence microscopy. Blue/turquoise, nuclear staining by DAPI; green, CD68 (MΦ) or CD11c (DC); red, CD14 (MΦ); gray/black, TRAP (OC).

See also Figure S2.

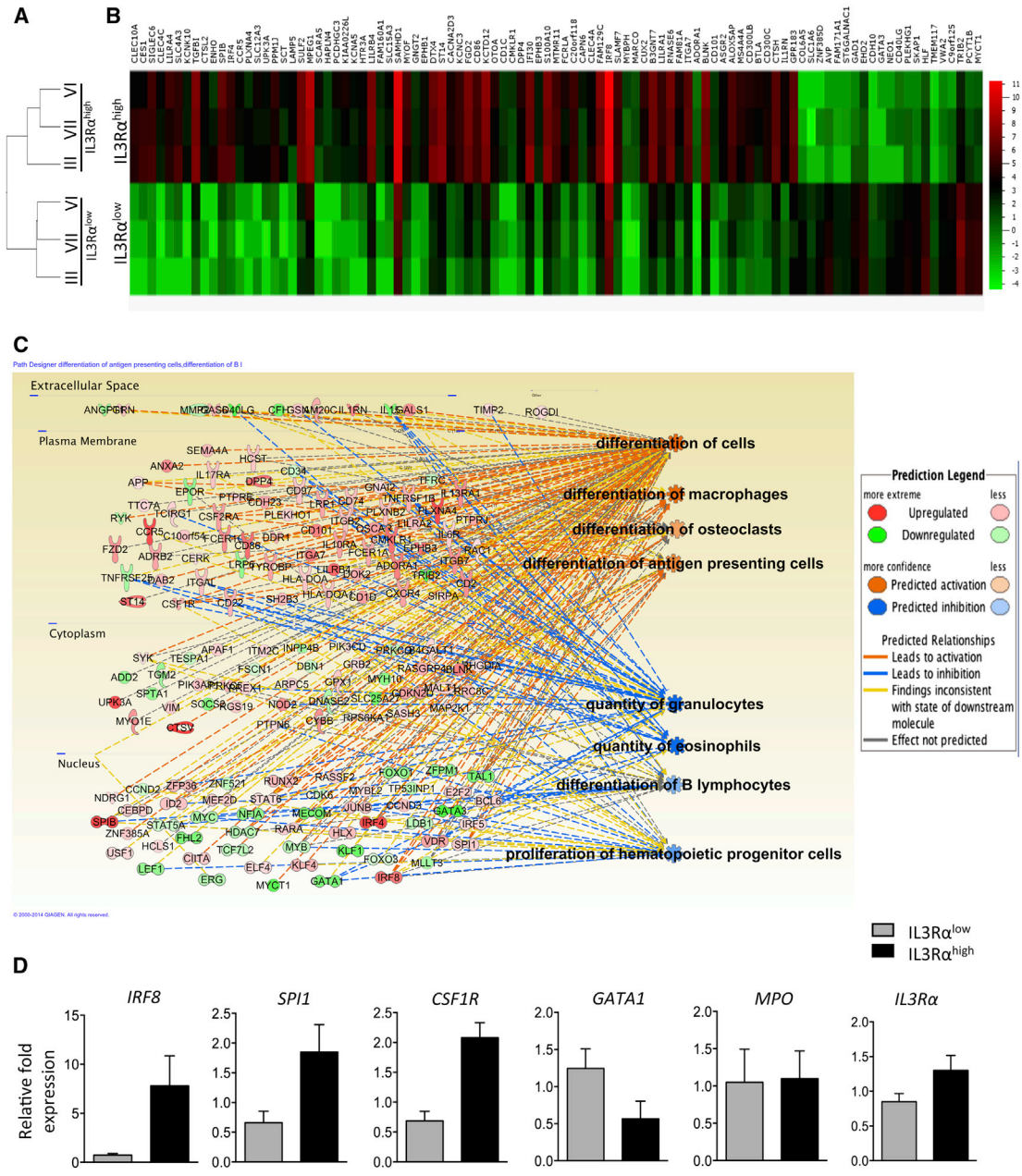

Figure 4. Transcriptomics Validates the Functional Definition of IL3Rα^{high} and IL3Rα^{low} CD11b^{-}CD34^{+}c-KIT^{+}FLT3^{+} BM Subsets and Their Relationship

IL3Rα^{high} and IL3Rα^{low} subsets were sorted from BM of donors III, VI, and VII and subjected to mRNA deep sequencing. Sequence reads were analyzed as indicated in the Supplemental Information.

(A) Hierarchical clustering of all protein-coding genes from the different samples.

(B) Heatmap, made with Qlucore software including 97 genes with the highest differential expression ($p < 0.001$; $\log_2$-fold change > 3.5 or < −3.5). Upregulated and downregulated genes are ordered separately according to the degree of differential expression (from "high" to "low"). The scale bar denotes expression level as $\log_2$ value.

(C) Results are depicted of IPA of 649 genes found to be differentially expressed at $p < 0.001$. The IPA network: extracellular, plasma membrane, cytoplasmic, and nuclear molecules with higher mRNA expression in the IL3Rα^{high} subset are depicted in shades of red (positive $\log_2$ ratios) and molecules with lower mRNA expression in shades of green (negative $\log_2$ ratios). The molecules depicted cluster in the listed functional categories of genes as identified by IPA.

(D) Validation of a selection of molecules by qPCR on mRNA (mean + SEM; three donors).

SUPPLEMENTAL INFORMATION

Supplemental Information includes Supplemental Experimental Procedures, two figures, and three tables and can be found with this article online at http://dx.doi.org/10.1016/j.stemcr.2015.04.012.

AUTHOR CONTRIBUTIONS

Y.X. designed and performed research, analyzed data, and wrote the paper; S.Z. designed and performed experiments, analyzed data, and contributed to writing of the paper; L.W. and D.C.d.G. performed experiments and analyzed data; M.J.v.T. and A.C.L. provided clinical samples, analyzed data, and provided critical comments; and J.B. analyzed data, provided insight, and wrote the paper.

ACKNOWLEDGMENTS

The authors thank E. de Vries, N. Pan, F. van Diepen, A. Pfauth, C. Bachas, L. Brocks, L. Oomen, I. de Rink, A. Velds, Y.-Y. Chen, and R. Kerkhoven for experimental assistance and advice and the Landsteiner Foundation for Blood Transfusion Research for financial support.

Received: September 24, 2014
Revised: April 22, 2015
Accepted: April 23, 2015
Published: May 21, 2015

REFERENCES

Adolfsson, J., Månsson, R., Buza-Vidas, N., Hultquist, A., Liuba, K., Jensen, C.T., Bryder, D., Yang, L., Borge, O.J., Thoren, L.A., et al. (2005). Identification of Flt3+ lympho-myeloid stem cells lacking erythro-megakaryocytic potential a revised road map for adult blood lineage commitment. Cell *121*, 295–306.

Arai, F., Miyamoto, T., Ohneda, O., Inada, T., Sudo, T., Brasel, K., Miyata, T., Anderson, D.M., and Suda, T. (1999). Commitment and differentiation of osteoclast precursor cells by the sequential expression of c-Fms and receptor activator of nuclear factor kappaB (RANK) receptors. J. Exp. Med. *190*, 1741–1754.

Balan, S., Ollion, V., Colletti, N., Chelbi, R., Montanana-Sanchis, F., Liu, H., Vu Manh, T.P., Sanchez, C., Savoret, J., Perrot, I., et al. (2014). Human XCR1+ dendritic cells derived in vitro from CD34+ progenitors closely resemble blood dendritic cells, including their adjuvant responsiveness, contrary to monocyte-derived dendritic cells. J. Immunol. *193*, 1622–1635.

Belz, G.T., and Nutt, S.L. (2012). Transcriptional programming of the dendritic cell network. Nat. Rev. Immunol. *12*, 101–113.

Choi, K.-D., Vodyanik, M.A., and Slukvin, I.I. (2009). Generation of mature human myelomonocytic cells through expansion and differentiation of pluripotent stem cell-derived lin-CD34+ CD43+CD45+ progenitors. J. Clin. Invest. *119*, 2818–2829.

Chomarat, P., Banchereau, J., Davoust, J., and Palucka, A.K. (2000). IL-6 switches the differentiation of monocytes from dendritic cells to macrophages. Nat. Immunol. *1*, 510–514.

Doulatov, S., Notta, F., Eppert, K., Nguyen, L.T., Ohashi, P.S., and Dick, J.E. (2010). Revised map of the human progenitor hierarchy shows the origin of macrophages and dendritic cells in early lymphoid development. Nat. Immunol. *11*, 585–593.

Doulatov, S., Notta, F., Laurenti, E., and Dick, J.E. (2012). Hematopoiesis: a human perspective. Cell Stem Cell *10*, 120–136.

Goardon, N., Marchi, E., Atzberger, A., Quek, L., Schuh, A., Soneji, S., Woll, P., Mead, A., Alford, K.A., Rout, R., et al. (2011). Coexistence of LMPP-like and GMP-like leukemia stem cells in acute myeloid leukemia. Cancer Cell *19*, 138–152.

Görgens, A., Radtke, S., Möllmann, M., Cross, M., Dürig, J., Horn, P.A., and Giebel, B. (2013). Revision of the human hematopoietic tree: granulocyte subtypes derive from distinct hematopoietic lineages. Cell Rep. *3*, 1539–1552.

Hettinger, J., Richards, D.M., Hansson, J., Barra, M.M., Joschko, A.-C., Krijgsveld, J., and Feuerer, M. (2013). Origin of monocytes and macrophages in a committed progenitor. Nat. Immunol. *14*, 821–830.

Jacome-Galarza, C.E., Lee, S.K., Lorenzo, J.A., and Aguila, H.L. (2013). Identification, characterization, and isolation of a common progenitor for osteoclasts, macrophages, and dendritic cells from murine bone marrow and periphery. J. Bone Miner. Res. *28*, 1203–1213.

Kawamoto, H., Ikawa, T., Masuda, K., Wada, H., and Katsura, Y. (2010). A map for lineage restriction of progenitors during hematopoiesis: the essence of the myeloid-based model. Immunol. Rev. *238*, 23–36.

Lawrence, T., and Natoli, G. (2011). Transcriptional regulation of macrophage polarization: enabling diversity with identity. Nat. Rev. Immunol. *11*, 750–761.

Lee, J., Breton, G., Oliveira, T.Y., Zhou, Y.J., Aljoufi, A., Puhr, S., Cameron, M.J., Sékaly, R.P., Nussenzweig, M.C., and Liu, K. (2015). Restricted dendritic cell and monocyte progenitors in human cord blood and bone marrow. J. Exp. Med. *212*, 385–399.

Liu, K., and Nussenzweig, M.C. (2010). Origin and development of dendritic cells. Immunol. Rev. *234*, 45–54.

MacDonald, K.P.A., Munster, D.J., Clark, G.J., Dzionek, A., Schmitz, J., and Hart, D.N.J. (2002). Characterization of human blood dendritic cell subsets. Blood *100*, 4512–4520.

Manz, M.G., Miyamoto, T., Akashi, K., and Weissman, I.L. (2002). Prospective isolation of human clonogenic common myeloid progenitors. Proc. Natl. Acad. Sci. USA *99*, 11872–11877.

McKenna, H.J., Stocking, K.L., Miller, R.E., Brasel, K., De Smedt, T., Maraskovsky, E., Maliszewski, C.R., Lynch, D.H., Smith, J., Pulendran, B., et al. (2000). Mice lacking flt3 ligand have deficient hematopoiesis affecting hematopoietic progenitor cells, dendritic cells, and natural killer cells. Blood *95*, 3489–3497.

Miyamoto, T., Ohneda, O., Arai, F., Iwamoto, K., Okada, S., Takagi, K., Anderson, D.M., and Suda, T. (2001). Bifurcation of osteoclasts and dendritic cells from common progenitors. Blood *98*, 2544–2554.

Mori, Y., Iwasaki, H., Kohno, K., Yoshimoto, G., Kikushige, Y., Okeda, A., Uike, N., Niiro, H., Takenaka, K., Nagafuji, K., et al. (2009). Identification of the human eosinophil lineage-committed

progenitor: revision of phenotypic definition of the human common myeloid progenitor. J. Exp. Med. *206*, 183–193.

Rosenbauer, F., and Tenen, D.G. (2007). Transcription factors in myeloid development: balancing differentiation with transformation. Nat. Rev. Immunol. *7*, 105–117.

Takayanagi, H. (2007). Osteoimmunology: shared mechanisms and crosstalk between the immune and bone systems. Nat. Rev. Immunol. *7*, 292–304.

Theill, L.E., Boyle, W.J., and Penninger, J.M. (2002). RANK-L and RANK: T cells, bone loss, and mammalian evolution. Annu. Rev. Immunol. *20*, 795–823.

Vieira, P., and Cumano, A. (2004). Differentiation of B lymphocytes from hematopoietic stem cells. Methods Mol. Biol. *271*, 67–76.

Walsh, M.C., Kim, N., Kadono, Y., Rho, J., Lee, S.Y., Lorenzo, J., and Choi, Y. (2006). Osteoimmunology: interplay between the immune system and bone metabolism. Annu. Rev. Immunol. *24*, 33–63.

Weissman, I.L., and Shizuru, J.A. (2008). The origins of the identification and isolation of hematopoietic stem cells, and their capability to induce donor-specific transplantation tolerance and treat autoimmune diseases. Blood *112*, 3543–3553.

Xiao, Y., Song, J.-Y., de Vries, T.J., Fatmawati, C., Parreira, D.B., Langenbach, G.E., Babala, N., Nolte, M.A., Everts, V., and Borst, J. (2013). Osteoclast precursors in murine bone marrow express CD27 and are impeded in osteoclast development by CD70 on activated immune cells. Proc. Natl. Acad. Sci. USA *110*, 12385–12390.